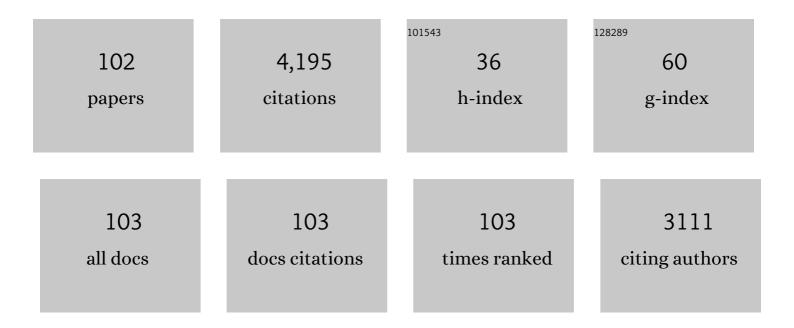
Tao Cheng

List of Publications by Year in descending order

Source: https://exaly.com/author-pdf/4398991/publications.pdf Version: 2024-02-01



TAO CHENC

#	Article	IF	CITATIONS
1	Development of critical nitrogen dilution curves for different leaf layers within the rice canopy. European Journal of Agronomy, 2022, 132, 126414.	4.1	8
2	Combining spectral and texture features of UAV hyperspectral images for leaf nitrogen content monitoring in winter wheat. International Journal of Remote Sensing, 2022, 43, 2335-2356.	2.9	15
3	MACA: A Relative Radiometric Correction Method for Multiflight Unmanned Aerial Vehicle Images Based on Concurrent Satellite Imagery. IEEE Transactions on Geoscience and Remote Sensing, 2022, 60, 1-14.	6.3	6
4	An assessment of background removal approaches for improved estimation of rice leaf nitrogen concentration with unmanned aerial vehicle multispectral imagery at various observation times. Field Crops Research, 2022, 283, 108543.	5.1	18
5	Advances in the estimations and applications of critical nitrogen dilution curve and nitrogen nutrition index of major cereal crops. A review. Computers and Electronics in Agriculture, 2022, 197, 106998.	7.7	20
6	An assessment of multi-view spectral information from UAV-based color-infrared images for improved estimation of nitrogen nutrition status in winter wheat. Precision Agriculture, 2022, 23, 1653-1674.	6.0	9
7	Hyperspectral Reflectance Proxies to Diagnose In-Field Fusarium Head Blight in Wheat with Machine Learning. Remote Sensing, 2022, 14, 2784.	4.0	13
8	Next Step in Vegetation Remote Sensing: Synergetic Retrievals of Canopy Structural and Leaf Biochemical Parameters. , 2022, , 207-220.		3
9	Evaluation of Diverse Convolutional Neural Networks and Training Strategies for Wheat Leaf Disease Identification with Field-Acquired Photographs. Remote Sensing, 2022, 14, 3446.	4.0	24
10	Estimation of rice plant potassium accumulation based on non-negative matrix factorization using hyperspectral reflectance. Precision Agriculture, 2021, 22, 51-74.	6.0	17
11	Estimation of leaf nitrogen content and photosynthetic nitrogen use efficiency in wheat using sun-induced chlorophyll fluorescence at the leaf and canopy scales. European Journal of Agronomy, 2021, 122, 126192.	4.1	41
12	Detection of Urban Built-Up Area Change From Sentinel-2 Images Using Multiband Temporal Texture and One-Class Random Forest. IEEE Journal of Selected Topics in Applied Earth Observations and Remote Sensing, 2021, 14, 6974-6986.	4.9	11
13	Estimating the Leaf Nitrogen Content with a New Feature Extracted from the Ultra-High Spectral and Spatial Resolution Images in Wheat. Remote Sensing, 2021, 13, 739.	4.0	11
14	Laboratory shortwave infrared reflectance spectroscopy for estimating grain protein content in rice and wheat. International Journal of Remote Sensing, 2021, 42, 4467-4492.	2.9	3
15	Leaf area index estimation model for UAV image hyperspectral data based on wavelength variable selection and machine learning methods. Plant Methods, 2021, 17, 49.	4.3	66
16	Spectroscopic detection of rice leaf blast infection from asymptomatic to mild stages with integrated machine learning and feature selection. Remote Sensing of Environment, 2021, 257, 112350.	11.0	55
17	An assessment of Planet satellite imagery for county-wide mapping of rice planting areas in Jiangsu Province, China with one-class classification approaches. International Journal of Remote Sensing, 2021, 42, 7610-7635.	2.9	5
18	Combining Remote Sensing and Meteorological Data for Improved Rice Plant Potassium Content Estimation. Remote Sensing, 2021, 13, 3502.	4.0	5

#	Article	IF	CITATIONS
19	Early Detection of Powdery Mildew Disease and Accurate Quantification of Its Severity Using Hyperspectral Images in Wheat. Remote Sensing, 2021, 13, 3612.	4.0	27
20	AGTOC: A novel approach to winter wheat mapping by automatic generation of training samples and one-class classification on Google Earth Engine. International Journal of Applied Earth Observation and Geoinformation, 2021, 102, 102446.	2.8	16
21	Retrieving potassium levels in wheat blades using normalised spectra. International Journal of Applied Earth Observation and Geoinformation, 2021, 102, 102412.	2.8	4
22	AAVI: A Novel Approach to Estimating Leaf Nitrogen Concentration in Rice From Unmanned Aerial Vehicle Multispectral Imagery at Early and Middle Growth Stages. IEEE Journal of Selected Topics in Applied Earth Observations and Remote Sensing, 2021, 14, 6716-6728.	4.9	15
23	Estimation of Crop Yield From Combined Optical and SAR Imagery Using Gaussian Kernel Regression. IEEE Journal of Selected Topics in Applied Earth Observations and Remote Sensing, 2021, 14, 10520-10534.	4.9	26
24	Improving Unmanned Aerial Vehicle (UAV) remote sensing of rice plant potassium accumulation by fusing spectral and textural information. International Journal of Applied Earth Observation and Geoinformation, 2021, 104, 102592.	2.8	10
25	Monitoring leaf potassium content using hyperspectral vegetation indices in rice leaves. Precision Agriculture, 2020, 21, 324-348.	6.0	42
26	DESTIN: A new method for delineating the boundaries of crop fields by fusing spatial and temporal information from WorldView and Planet satellite imagery. Computers and Electronics in Agriculture, 2020, 178, 105787.	7.7	28
27	An automatic method for counting wheat tiller number in the field with terrestrial LiDAR. Plant Methods, 2020, 16, 132.	4.3	13
28	Improved estimation of leaf chlorophyll content of row crops from canopy reflectance spectra through minimizing canopy structural effects and optimizing off-noon observation time. Remote Sensing of Environment, 2020, 248, 111985.	11.0	70
29	Estimation of Canopy Biomass Components in Paddy Rice from Combined Optical and SAR Data Using Multi-Target Gaussian Regressor Stacking. Remote Sensing, 2020, 12, 2564.	4.0	25
30	HISTIF: A New Spatiotemporal Image Fusion Method for High-Resolution Monitoring of Crops at the Subfield Level. IEEE Journal of Selected Topics in Applied Earth Observations and Remote Sensing, 2020, 13, 4607-4626.	4.9	19
31	Estimating aboveground and organ biomass of plant canopies across the entire season of rice growth with terrestrial laser scanning. International Journal of Applied Earth Observation and Geoinformation, 2020, 91, 102132.	2.8	28
32	Enhancing the Nitrogen Signals of Rice Canopies across Critical Growth Stages through the Integration of Textural and Spectral Information from Unmanned Aerial Vehicle (UAV) Multispectral Imagery. Remote Sensing, 2020, 12, 957.	4.0	44
33	Monitoring daily variation of leaf layer photosynthesis in rice using UAV-based multi-spectral imagery and a light response curve model. Agricultural and Forest Meteorology, 2020, 291, 108098.	4.8	24
34	Early season detection of rice plants using RGB, NIR-G-B and multispectral images from unmanned aerial vehicle (UAV). Computers and Electronics in Agriculture, 2020, 169, 105223.	7.7	49
35	Detection of phenology using an improved shape model on time-series vegetation index in wheat. Computers and Electronics in Agriculture, 2020, 173, 105398.	7.7	31
36	Generating Red-Edge Images at 3 M Spatial Resolution by Fusing Sentinel-2 and Planet Satellite Products. Remote Sensing, 2019, 11, 1422.	4.0	21

#	Article	IF	CITATIONS
37	Combining Color Indices and Textures of UAV-Based Digital Imagery for Rice LAI Estimation. Remote Sensing, 2019, 11, 1763.	4.0	126
38	Estimating Leaf Area Index with a New Vegetation Index Considering the Influence of Rice Panicles. Remote Sensing, 2019, 11, 1809.	4.0	29
39	Detection of wheat height using optimized multi-scan mode of LiDAR during the entire growth stages. Computers and Electronics in Agriculture, 2019, 165, 104959.	7.7	29
40	A newly developed method to extract the optimal hyperspectral feature for monitoring leaf biomass in wheat. Computers and Electronics in Agriculture, 2019, 165, 104942.	7.7	29
41	Combining computer vision and deep learning to enable ultra-scale aerial phenotyping and precision agriculture: A case study of lettuce production. Horticulture Research, 2019, 6, 70.	6.3	105
42	Assessment of unified models for estimating leaf chlorophyll content across directional-hemispherical reflectance and bidirectional reflectance spectra. Remote Sensing of Environment, 2019, 231, 111240.	11.0	40
43	Inversion of rice canopy chlorophyll content and leaf area index based on coupling of radiative transfer and Bayesian network models. ISPRS Journal of Photogrammetry and Remote Sensing, 2019, 150, 185-196.	11.1	83
44	Predicting wheat productivity: Integrating time series of vegetation indices into crop modeling via sequential assimilation. Agricultural and Forest Meteorology, 2019, 272-273, 69-80.	4.8	52
45	Improved estimation of aboveground biomass in wheat from RGB imagery and point cloud data acquired with a low-cost unmanned aerial vehicle system. Plant Methods, 2019, 15, 17.	4.3	117
46	Analysis and Evaluation of the Image Preprocessing Process of a Six-Band Multispectral Camera Mounted on an Unmanned Aerial Vehicle for Winter Wheat Monitoring. Sensors, 2019, 19, 747.	3.8	16
47	Using Digital Cameras on an Unmanned Aerial Vehicle to Derive Optimum Color Vegetation Indices for Leaf Nitrogen Concentration Monitoring in Winter Wheat. Remote Sensing, 2019, 11, 2667.	4.0	27
48	Exploiting the Textural Information of UAV Multispectral Imagery to Monitor Nitrogen Status in Rice. , 2019, , .		2
49	Estimation of Nitrogen Nutrition Status in Winter Wheat From Unmanned Aerial Vehicle Based Multi-Angular Multispectral Imagery. Frontiers in Plant Science, 2019, 10, 1601.	3.6	47
50	Evaluation of Aboveground Nitrogen Content of Winter Wheat Using Digital Imagery of Unmanned Aerial Vehicles. Sensors, 2019, 19, 4416.	3.8	38
51	Quantifying Chlorophyll Fluorescence Parameters from Hyperspectral Reflectance at the Leaf Scale under Various Nitrogen Treatment Regimes in Winter Wheat. Remote Sensing, 2019, 11, 2838.	4.0	33
52	Comparison of the abilities of vegetation indices and photosynthetic parameters to detect heat stress in wheat. Agricultural and Forest Meteorology, 2019, 265, 121-136.	4.8	33
53	Improved estimation of rice aboveground biomass combining textural and spectral analysis of UAV imagery. Precision Agriculture, 2019, 20, 611-629.	6.0	171
54	Estimation of Vertical Leaf Nitrogen Distribution Within a Rice Canopy Based on Hyperspectral Data. Frontiers in Plant Science, 2019, 10, 1802.	3.6	23

#	Article	IF	CITATIONS
55	Integrating remote sensing information with crop model to monitor wheat growth and yield based on simulation zone partitioning. Precision Agriculture, 2018, 19, 55-78.	6.0	45
56	PROCWT: Coupling PROSPECT with continuous wavelet transform to improve the retrieval of foliar chemistry from leaf bidirectional reflectance spectra. Remote Sensing of Environment, 2018, 206, 1-14.	11.0	63
57	Improved Estimation of Leaf Chlorophyll Content from Non-Noon Reflectance Spectra of Wheat Canopies by Avoiding the Effect of Soil Background. , 2018, , .		0
58	BRDF Effect on the Estimation of Canopy Chlorophyll Content in Paddy Rice from UAV-Based Hyperspectral Imagery. , 2018, , .		5
59	Power and Difference of the Up-and-Downward Sun-Induced Chlorophyll Fluorescence on Detecting Leaf Nitrogen Content in Wheat at the Leaf Scale. , 2018, , .		0
60	Detecting Rice Blast Disease Using Model Inverted Biochemical Variables from Close-Range Reflectance Imagery of Fresh Leaves. , 2018, , .		3
61	A Comparative Assessment of Different Modeling Algorithms for Estimating Leaf Nitrogen Content in Winter Wheat Using Multispectral Images from an Unmanned Aerial Vehicle. Remote Sensing, 2018, 10, 2026.	4.0	84
62	Improving the Estimation of Leaf Area Index in Winter Wheat at Regional Scale. , 2018, , .		0
63	Potential of UAV-Based Active Sensing for Monitoring Rice Leaf Nitrogen Status. Frontiers in Plant Science, 2018, 9, 1834.	3.6	45
64	Hyperspectral Estimation of Canopy Leaf Biomass Phenotype per Ground Area Using a Continuous Wavelet Analysis in Wheat. Frontiers in Plant Science, 2018, 9, 1360.	3.6	24
65	Difference and Potential of the Upward and Downward Sun-Induced Chlorophyll Fluorescence on Detecting Leaf Nitrogen Concentration in Wheat. Remote Sensing, 2018, 10, 1315.	4.0	12
66	Assessing the Impact of Spatial Resolution on the Estimation of Leaf Nitrogen Concentration Over the Full Season of Paddy Rice Using Near-Surface Imaging Spectroscopy Data. Frontiers in Plant Science, 2018, 9, 964.	3.6	69
67	Estimation of area- and mass-based leaf nitrogen contents of wheat and rice crops from water-removed spectra using continuous wavelet analysis. Plant Methods, 2018, 14, 76.	4.3	55
68	Combining Unmanned Aerial Vehicle (UAV)-Based Multispectral Imagery and Ground-Based Hyperspectral Data for Plant Nitrogen Concentration Estimation in Rice. Frontiers in Plant Science, 2018, 9, 936.	3.6	86
69	Evaluation of Three Techniques for Correcting the Spatial Scaling Bias of Leaf Area Index. Remote Sensing, 2018, 10, 221.	4.0	15
70	Evaluation of One-Class Support Vector Classification for Mapping the Paddy Rice Planting Area in Jiangsu Province of China from Landsat 8 OLI Imagery. Remote Sensing, 2018, 10, 546.	4.0	23
71	Evaluation of RGB, Color-Infrared and Multispectral Images Acquired from Unmanned Aerial Systems for the Estimation of Nitrogen Accumulation in Rice. Remote Sensing, 2018, 10, 824.	4.0	115
72	Development and testing of an ear-leaf model for rice canopy reflectance. Journal of Applied Remote Sensing, 2018, 12, 1.	1.3	1

#	Article	IF	CITATIONS
73	A new spectral similarity water index for the estimation of leaf water content from hyperspectral data of leaves. Remote Sensing of Environment, 2017, 196, 13-27.	11.0	39
74	WREP: A wavelet-based technique for extracting the red edge position from reflectance spectra for estimating leaf and canopy chlorophyll contents of cereal crops. ISPRS Journal of Photogrammetry and Remote Sensing, 2017, 129, 103-117.	11.1	65
75	Predicting grain yield in rice using multi-temporal vegetation indices from UAV-based multispectral and digital imagery. ISPRS Journal of Photogrammetry and Remote Sensing, 2017, 130, 246-255.	11.1	395
76	A new three-band spectral index for mitigating the saturation in the estimation of leaf area index in wheat. International Journal of Remote Sensing, 2017, 38, 3865-3885.	2.9	31
77	Estimation of Wheat LAI at Middle to High Levels Using Unmanned Aerial Vehicle Narrowband Multispectral Imagery. Remote Sensing, 2017, 9, 1304.	4.0	102
78	Spectroscopic Estimation of Biomass in Canopy Components of Paddy Rice Using Dry Matter and Chlorophyll Indices. Remote Sensing, 2017, 9, 319.	4.0	46
79	Assessing the Spectral Properties of Sunlit and Shaded Components in Rice Canopies with Near-Ground Imaging Spectroscopy Data. Sensors, 2017, 17, 578.	3.8	25
80	Preface: Recent Advances in Remote Sensing for Crop Growth Monitoring. Remote Sensing, 2016, 8, 116.	4.0	12
81	Retrieval of LEAF pigment content using wavelet-based prospect inversion from leaf reflectance spectra. , 2016, , .		0
82	Estimating wheat yield by integrating the WheatGrow and PROSAIL models. Field Crops Research, 2016, 192, 55-66.	5.1	30
83	Monitoring leaf area index after heading stage using hyperspectral remote sensing data in rice. , 2016, ,		2
84	Detection of rice phenology through time series analysis of ground-based spectral index data. Field Crops Research, 2016, 198, 131-139.	5.1	84
85	Comparative analysis of vegetation indices, non-parametric and physical retrieval methods for monitoring nitrogen in wheat using UAV-based multispectral imagery. , 2016, , .		14
86	Mapping rice planting area from Landsat 8 imagery using one-class support vector machine. , 2016, , .		1
87	Assessment of spectral variation between rice canopy components using spectral feature analysis of near-ground hyperspectral imaging data. , 2016, , .		4
88	Wavelet-based PROSPECT inversion for retrieving leaf mass per area (LMA) and equivalent water thickness (EWT) from leaf reflectance. , 2016, , .		2
89	Evaluation of Six Algorithms to Monitor Wheat Leaf Nitrogen Concentration. Remote Sensing, 2015, 7, 14939-14966.	4.0	99
90	A wavelet-based technique for extracting the red edge position from vegetation reflectance spectra. , 2015, , .		0

#	Article	IF	CITATIONS
91	Comparison of Different Hyperspectral Vegetation Indices for Estimating Canopy Leaf Nitrogen Accumulation in Rice. Agronomy Journal, 2014, 106, 1911-1920.	1.8	15
92	Detecting diurnal and seasonal variation in canopy water content of nut tree orchards from airborne imaging spectroscopy data using continuous wavelet analysis. Remote Sensing of Environment, 2014, 143, 39-53.	11.0	63
93	Deriving leaf mass per area (LMA) from foliar reflectance across a variety of plant species using continuous wavelet analysis. ISPRS Journal of Photogrammetry and Remote Sensing, 2014, 87, 28-38.	11.1	101
94	Detecting leaf nitrogen content in wheat with canopy hyperspectrum under different soil backgrounds. International Journal of Applied Earth Observation and Geoinformation, 2014, 32, 114-124.	2.8	45
95	Detection of diurnal variation in orchard canopy water content using MODIS/ASTER airborne simulator (MASTER) data. Remote Sensing of Environment, 2013, 132, 1-12.	11.0	27
96	Predicting leaf gravimetric water content from foliar reflectance across a range of plant species using continuous wavelet analysis. Journal of Plant Physiology, 2012, 169, 1134-1142.	3.5	86
97	Land cover classification using CHRIS/PROBA images and multi-temporal texture. International Journal of Remote Sensing, 2012, 33, 101-119.	2.9	17
98	Insect outbreaks produce distinctive carbon isotope signatures in defensive resins and fossiliferous ambers. Proceedings of the Royal Society B: Biological Sciences, 2011, 278, 3219-3224.	2.6	40
99	Spectroscopic determination of leaf water content using continuous wavelet analysis. Remote Sensing of Environment, 2011, 115, 659-670.	11.0	210
100	Continuous wavelet analysis for the detection of green attack damage due to mountain pine beetle infestation. Remote Sensing of Environment, 2010, 114, 899-910.	11.0	141
101	Multivariate Image Texture by Multivariate Variogram for Multispectral Image Classification. Photogrammetric Engineering and Remote Sensing, 2009, 75, 147-157.	0.6	28
102	Lithologic mapping using ASTER imagery and multivariate texture. Canadian Journal of Remote Sensing, 2009, 35, S117-S125.	2.4	3